Solar Energy Materials & Solar Cells 259 (2023) 112435

Contents lists available at ScienceDirect

Solar Energy Materials and Solar Cells

journal homepage: www.elsevier.com/locate/solmat

Metamorphic front- and rear-junction 1.7 eV GaInP solar cells with high open-circuit voltage

Mijung Kim [a,b], Yukun Sun [a,b], Ryan D. Hool [b,c], Minjoo Larry Lee [a,b,*]

[a] Department of Electrical and Computer Engineering, University of Illinois Urbana-Champaign, Urbana, IL, 61801, USA
[b] Nick Holonyak, Jr. Micro and Nanotechnology Laboratory, University of Illinois Urbana-Champaign, Urbana, IL, 61801, USA
[c] Department of Materials Science and Engineering, University of Illinois Urbana-Champaign, Urbana, IL, 61801, USA

ARTICLE INFO

Keywords:
MBE
Metamorphic solar cells
Rapid thermal annealing
GaInP
Rear-heterojunction

ABSTRACT

1.7 eV absorber materials are important in high-performance III-V multi-junction solar cells. Here, we show that rapid thermal annealing significantly improves the carrier lifetimes in lightly doped metamorphic 1.7 eV $Ga_{0.37}In_{0.63}P$ (MM GaInP) grown on GaAs by molecular beam epitaxy. A low threading dislocation density of ~6 × 10^5 cm^{-2} was achieved through the use of an $In_xGa_{1-x}As$ graded buffer. Annealing enables minority carrier lifetimes in 1.7 eV *p*- and *n*-GaInP of 3.9 and 28 ns, respectively, both of which are higher than annealed lattice-matched 1.9 eV $Ga_{0.51}In_{0.49}P$ (LM GaInP) grown in the same chamber. With the benefit of annealing, MM 1.7 eV GaInP front-junction solar cells show a high peak internal quantum efficiency of 94.3% and an open-circuit voltage (V_{OC}) of 1.17 V. We also demonstrate the first MM 1.7 eV GaInP rear-heterojunction cells with high fill factor and V_{OC} of 85% and 1.21 V, respectively, by taking advantage of long carrier lifetime while eliminating majority carrier blocking. The high V_{OC} values for the 1.7 eV GaInP cells presented in this work indicate promising tolerance to threading dislocations in MM GaInP.

1. Introduction

High-quality III-V absorbers with bandgap energy (E_g) of ~1.7 eV play an essential role in a wide variety of multi-junction solar cell designs. For example, 1.7 eV/1.1 eV dual-junction (2J) cells [1–4] have the potential for 3–4% higher efficiency than well-established 1.9 eV GaInP/1.4 eV GaAs 2J cells [5,6] due to better spectral matching [7], similar to what is attained by adding a 0.66 eV Ge junction to a conventional 2J device [8,9]. Recently, a spectrally matched 2J solar cell utilizing a lattice-matched (LM) 1.7 eV GaInAsP top cell and a metamorphic (MM) 1.1 eV InGaAs bottom cell was reported with an ultra-high efficiency of 32.6% [1,10]; the 2J record of 32.9% was obtained in a 1.9 eV GaInP/1.4 eV GaAs 2J that contains a multiple quantum well region as part of the GaAs junction [11].

Spectrally matched 2J cells can, in principle, be realized using MM 1.7 eV $(Al)_{0.03}Ga_{0.28}In_{0.69}P$/1.1 eV $In_{0.21}Ga_{0.79}As$ where the two junctions are internally lattice-matched at ~5.72–5.74 Å; i.e., both junctions are lattice-matched to each other despite being mismatched to the substrate. Unlike MM cell designs where graded buffers reside between junctions [1,2], a 1.7 eV (Al)GaInP/1.1 eV InGaAs tandem allows the possibility of reusing both the bulk GaAs substrate and $In_xGa_{1-x}As$ step-graded buffer ($In_xGa_{1-x}As$ GB) by lifting off [12,13] the tandem as a flexible thin film cell. While 1.7 eV GaInP has been investigated for upright metamorphic 3J devices on Ge [14,15], relatively few details on the growth, structural, and optical properties of the MM GaInP were given.

Growth of MM 1.7 eV (Al)GaInP cells by molecular beam epitaxy (MBE) is challenging due to elevated threading dislocation density (TDD) originating from the ~1.1% lattice mismatch with the underlying GaAs substrate. Graded buffers are widely used to obtain high-efficiency multi-junction cells [14,16] and are typically grown at 600–700 °C to maximize dislocation glide velocity and minimize TDD [17,18]. However, $In_xGa_{1-x}As$ growth in MBE is generally carried out at ~350–530 °C to minimize indium desorption [19–22], which historically led to higher TDD compared to $In_xGa_{1-x}As$ GBs grown by metalorganic chemical vapor deposition (MOCVD) at a higher temperature of 650–725 °C [18,23]. A TDD of ~1 × 10^5 cm^{-2} is predicted to have minimal impact on solar cell performance [24–26], while metamorphic cells typically have TDDs in the range of 1 × 10^6–1 × 10^7 cm^{-2} [1,27,28].

An additional challenge of MBE-grown phosphide materials is point defects caused by the lower substrate temperature of 460–500 °C [29,30] compared to the MOCVD substrate temperature of >600 °C [31,32].

* Corresponding author. Department of Electrical and Computer Engineering, University of Illinois Urbana-Champaign, Urbana, IL, 61801, USA.
E-mail address: mllee@illinois.edu (M.L. Lee).

https://doi.org/10.1016/j.solmat.2023.112435
Received 17 March 2023; Received in revised form 6 June 2023; Accepted 15 June 2023
Available online 5 July 2023

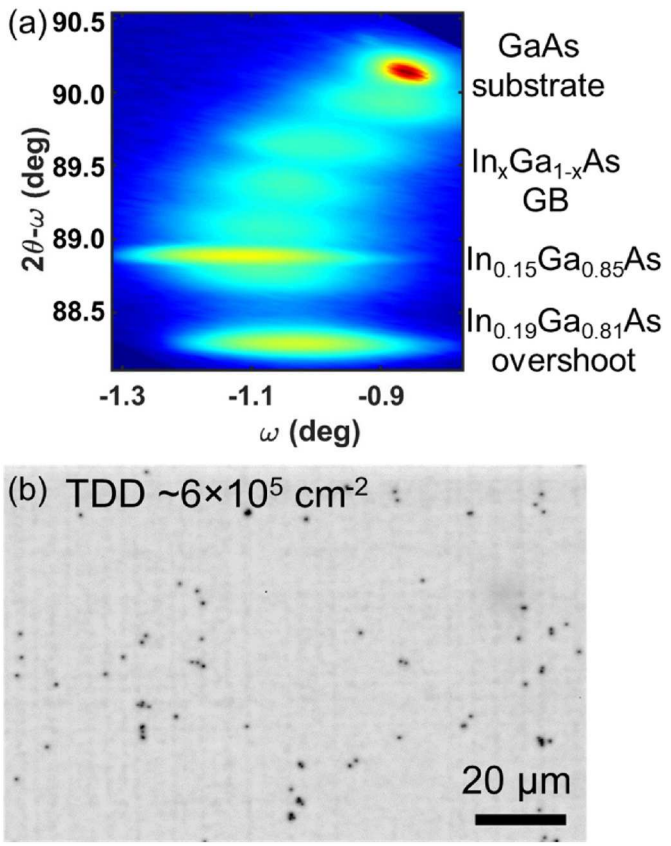

Fig. 1. (A) (115) reciprocal space map (RSM) of graded buffer with ~103% relaxation for $In_{0.15}Ga_{0.85}As$ cap layer. (b) EBIC image of MM 1.7 eV GaInP RHJ cell showing TDD of ~6 × 10^5 cm^{-2}.

Our previous work showed a significant performance improvement in MBE-grown LM $Ga_{0.51}In_{0.49}P$ and $(Al_xGa_{1-x})_{0.51}In_{0.49}P$ cells on GaAs by rapid thermal annealing (RTA) [30,33], enabling efficiencies similar to the best such devices grown by MOCVD. RTA also increased room temperature photoluminescence intensities and carrier lifetimes of lightly doped LM *p*- and *n*-GaInP double heterostructures (DHs), with concomitant improvement in open-circuit voltage (V_{OC}) of MBE-grown LM GaInP solar cells [30]. The mechanism of RTA enhancement in MBE-grown GaInP remains unclear. However, previously reported deep-level transient spectroscopy (DLTS) studies showed that annealing rearranged and reduced signals from point defects such as DX centers, O-related defects, and P vacancy-related defects in MBE-grown LM *n*-GaInP [34–38] and *p*-AlGaInP [39].

MOCVD- and MBE-grown GaInP rear-heterojunction (RHJ) cells have been demonstrated to have higher V_{OC} and external radiative efficiency than conventional front-junction (FJ) cells [30,31,40,41]. RHJ cells locate the space charge region (SCR) partially within a wider-E_g *p*-AlGaInP back surface field (BSF) at the rear of the devices, suppressing trap-assisted recombination within the depletion region, leading to lower dark current and improved V_{OC}. However, GaInP RHJ cells can suffer from poor carrier collection due to low hole mobilities (~18–40 cm^2/Vs) [42,43] and the need for relatively long hole diffusion lengths [41]. Another challenge of RHJ cells is insufficient front-side passivation due to Fermi-level pinning in the window layer caused by light doping (~1.0–5.0 × 10^{17} cm^{-3}) in the *n*-type emitter [30,44]. Our recent work showed that delta doping in the window layer boosted minority hole collection by preventing undesired band-bending [30]. In contrast, FJ *n* + *p* solar cells routinely achieve high short-circuit current density (J_{sc}) values despite relatively short minority carrier lifetimes because of the wide SCR located close to the front surface [40,41] and higher electron mobilities (~800–2000 cm^2/Vs) [42].

Fig. 2. Growth schematics of (a) MM *n*-GaInP DH with *n*-$In_{0.62}Al_{0.38}P$ barrier, (b) MM *p*-GaInP DH with 2.3 eV *p*-$Al_{0.33}Ga_{0.05}In_{0.62}P$ barrier on $In_xGa_{1-x}As$ GBs, (c) MM GaInP FJ cells, and (d) MM GaInP RHJ cells.

In this work, we investigated the effect of RTA on minority carrier lifetime in MM 1.7 eV *p*- and *n*-GaInP for use in FJ and RHJ solar cells, respectively. Lightly doped 1.7 eV *n*-GaInP exhibits a minority carrier lifetime of 28 ns after annealing, >2 × longer than LM 1.9 eV *n*-GaInP, despite threading dislocations. For lightly doped 1.7 eV *p*-GaInP, the carrier lifetime after RTA is 3.9 ns, which is also ~2 × longer than annealed LM *p*-GaInP grown by MBE. MM 1.7 eV GaInP FJ cells achieve high J_{SC} and a low bandgap-voltage offset ($W_{OC} = E_g/q\text{-}V_{OC}$) of 0.512 V, comparable to MBE-grown LM GaInP FJ cells. Additionally, we present the first MM 1.7 eV GaInP RHJ cells, attaining a low W_{OC} of 0.472 V and a high fill factor (FF) of 85.0% by improving series resistance and surface passivation by introducing a bridge layer between the BSF and buffer and adding delta-spikes in the window and emitter. The performance of our FJ and RHJ cells is promising for high-efficiency thin-film tandem cells with a spectrally matched E_g configuration of 1.7 eV/1.1 eV.

2. Experimental methods

All DHs and devices in this work were grown in a Veeco Mod GEN-II solid-source MBE system. To obtain the targeted lattice constant, 1.75 μm $In_xGa_{1-x}As$ GBs were grown on nominally on-axis GaAs (001) substrates at 500 °C with a grading rate of 0.63%/μm and a growth rate of 1.0–1.3 μm/h. The $In_xGa_{1-x}As$ GB was composed of 6 steps from x = 0.03 to 0.19, including an overshoot layer (250 nm for each step, 500 nm for the overshoot layer), followed by a fully relaxed $In_{0.15}Ga_{0.85}As$ cap layer (Fig. 1(a)). Electron beam-induced current (EBIC) mapping shows that we consistently attain low TDD <1 × 10^6 cm^{-2} in these layers, indicative of efficient dislocation glide kinetics despite using a low substrate temperature. Both MM GaInP FJ (not shown) and RHJ cells have low TDD of ~6 × 10^5 cm^{-2}, as revealed by EBIC (Fig. 1(b)).

Fig. 2(a) and (b) show growth schematics of 1.7 eV *n*- and *p*-GaInP DHs. Using the $In_xGa_{1-x}As$ GB as a template, DHs of 500 nm MM 1.7 eV GaInP with 100 nm MM *n*-$In_{0.62}Al_{0.38}P$ (InAlP) for *n*-type barriers (MM

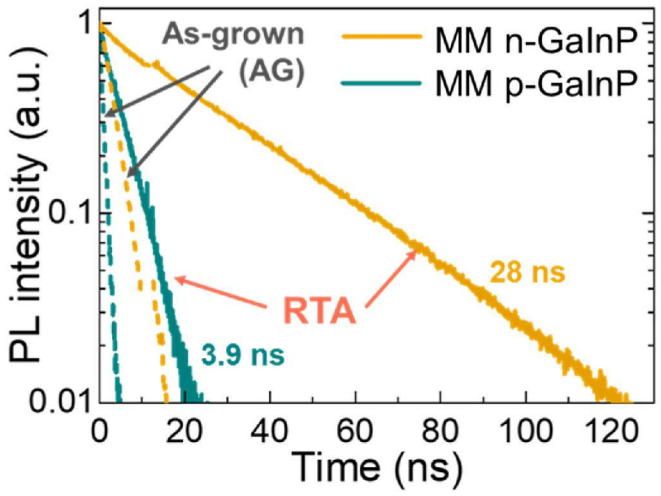

Fig. 3. TRPL decay curves of MM *n*- and *p*-GaInP DHs before and after RTA. MM *n*-GaInP DH has longer lifetime than MM *p*-GaInP DH.

Table 1
τ_{TRPL} of LM and MM GaInP.

Sample	As-grown	RTA'd
MM *p*-GaInP	0.9 ns	3.9 ns
LM *p*-GaInP	0.9 ns	1.9 ns
MM n-GaInP	3.0 ns	28.0 ns
LM n-GaInP	3.8 ns	12.2 ns

p-$Al_{0.33}Ga_{0.05}In_{0.62}P$ for *p*-type barriers) were grown at 460 °C for time-resolved photoluminescence (TRPL) studies. 1.7 eV GaInP layers were lightly doped with electron (hole) concentrations of n_o (p_o) = 1.0×10^{17} cm^{-3} using Si and Be as *n*- and *p*-type dopants; MM *n*-InAlP (MM *p*-$Al_{0.33}Ga_{0.05}In_{0.62}P$) barriers were doped with n_o (p_o) = 1.0×10^{18} cm^{-3}. TRPL measurements were conducted under low-level injection conditions using a 532 nm pulsed laser with a 1 mm diameter spot size, 2.5 mW average power, 6 ps pulse width, and 3.6 MHz repetition rate.

The growth structures of MM 1.7 eV GaInP FJ and RHJ solar cells are shown in Fig. 2(c) and (d), respectively. The FJ cells consist of a 100 nm 2.0 eV *p*-$Al_{0.19}Ga_{0.19}In_{0.62}P$ (AlGaInP) BSF, 50 nm *p*-GaInP with graded doping, 1450 nm *p*-GaInP base, 70 nm *n*-GaInP emitter, 20 nm *n*-InAlP window and 200 nm *n*-InGaAs contact. The RHJ cells comprise a 100 nm 2.0 eV *p*-AlGaInP BSF, 810 nm *n*-GaInP emitter, 20 nm *n*-InAlP window, and 200 nm *n*-InGaAs contact. Si delta doping spikes were introduced at the top 20 nm of the emitter and window layers to prevent surface Fermi level pinning [30]. A bridge layer ($p_o = 2.0 \times 10^{18}$ cm^{-3}) consisting of 50 nm 2.0 eV *p*-AlGaInP and 50 nm *p*-GaInP between the heavily *p*-doped buffer ($p_o = 4.0 \times 10^{18}$ cm^{-3}) and the lightly *p*-doped BSF (p_o = 1.0×10^{17} cm^{-3}) was necessary for RHJ cells to avoid majority hole blocking, as described below. Each layer's composition and carrier concentration were calibrated with high-resolution x-ray diffraction and Hall effect measurement, respectively.

RTA processes were conducted under N_2 ambient with a ramp rate of 20 °C/s. Optimal RTA conditions (850–1000 °C, 1–30s) before fabrication of the solar cells were chosen based on maximizing steady-state photoluminescence intensity, and no anti-reflection coatings were applied. Solar cells were fabricated as described in our previous works [45,46]. Lighted current-voltage (LIV) measurements were performed under approximate AM1.5G illumination with an ABET Technologies 10,500 solar simulator to determine V_{OC}, J_{SC}, voltage at maximum power (V_{MP}), current density at maximum power (J_{MP}), FF, and efficiency (η). External quantum efficiency (EQE) and specular reflectance (R) were taken with a PV Measurements QEX7 system; internal quantum efficiency (IQE) was estimated as IQE = EQE/(1-R). Suns-V_{OC}

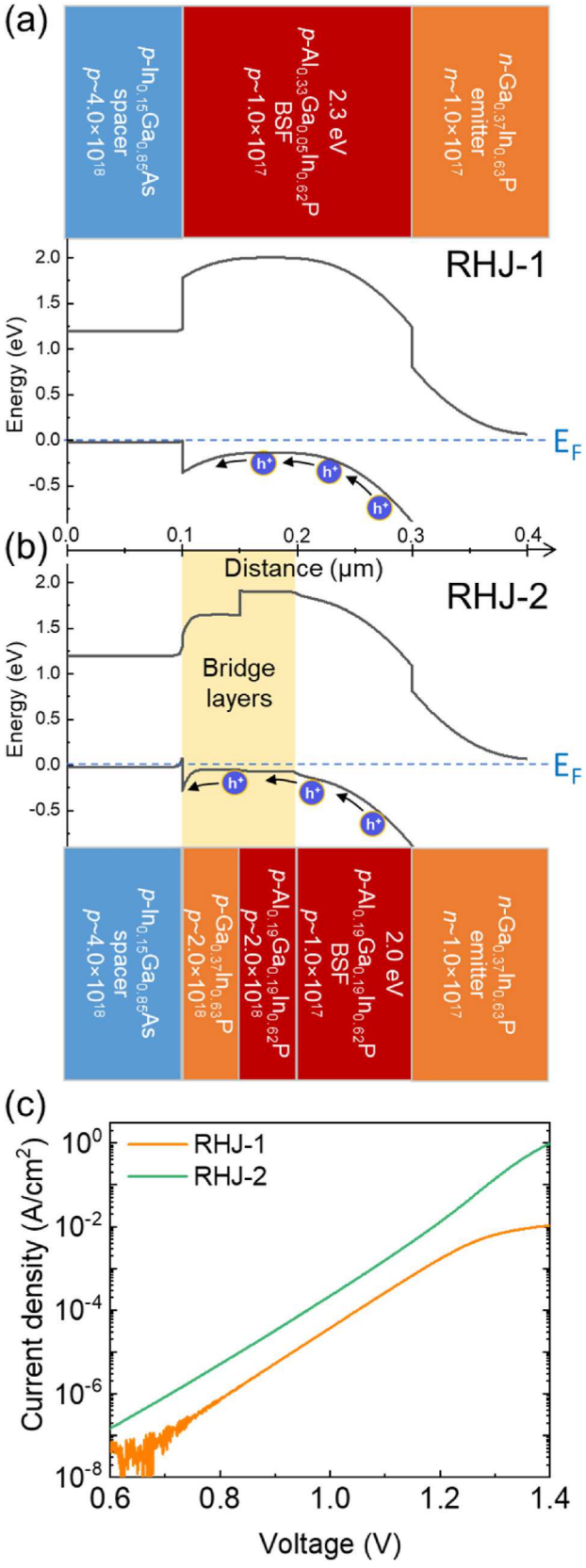

Fig. 4. Growth structures and band diagrams of (a) RHJ-1 without bridge layers and (b) RHJ-2 with bridge layers. Blue dashed lines indicate Fermi level (E_F). (c) DIV curves of RHJ-1 and RHJ-2. RHJ-1 showed a wider majority hole blocking barrier at the interface between BSF and spacer compared to RHJ-2.

Table 2
Effects of brige layers in RHJ cells.

Sample	Bridge layers	R_S (ohm-cm^2)	*FF difference (%)
RHJ-1	None	14.6	16.2
RHJ-2	50 nm AlGaInP+50 nm GaInP	1.1	0.2

All devices were annealed.

* FF difference (%): $\frac{|pFF - FF|}{FF} \times 100$.

measurements were conducted using a blue LED as a light source with dark currents J_{01} and J_{02} extracted using a MATLAB program. Series resistance (R_s) of solar cells was calculated using the following equation: $R_s = \frac{|V_{mp\ (Suns-V_{OC})} - V_{mp(LIV)}|}{J_{mp(LIV)}}$ [47]. Sheet resistance (R_{sheet}) and contact resistance ($R_{contact}$) of the fabricated cells were measured using the transfer length method (TLM), and band diagrams were simulated using Band-Prof software.

3. Results and discussion

3.1. RTA studies on MM GaInP DHs

TRPL decay curves of MM 1.7 eV *p*- and *n*-GaInP DHs demonstrate the improvement in minority carrier lifetimes by RTA (Fig. 3). TRPL lifetime (τ_{TRPL}) of the MM *p*-GaInP DH (Fig. 3, green lines) increased by 4 × and reached 3.9 ns after a 1000 °C 1s RTA. The relatively short τ_{TRPL} of MBE-grown *p*-GaInP [30] compared to MOCVD-grown LM *p*-GaInP (τ_{TRPL} ~29 ns) [48] suggests that Shockley-Read-Hall (SRH) recombination is the dominant recombination mechanism in our material; the radiative lifetime in LM GaInP with doping of 1.0×10^{17} cm^{-3} is ~50 ns [8]. Earlier reports showed that RTA could reduce the signal from O-related defects in LM *p*-AlGaInP [39], suggesting that annealing could similarly suppress defects in MM *p*-GaInP. Additional studies on Be-doped MM GaInP are needed to better understand the mechanism of RTA enhancement.

τ_{TRPL} of MM *n*-GaInP DHs (Fig. 3, orange lines) was dramatically improved by 9 × to 28 ns after RTA at 900 °C for 10s. Prior DLTS studies demonstrated a rearrangement of signals from O-related defects and decreased signals from DX centers and P vacancy-related defects in MBE-grown LM *n*-GaInP by annealing [34,36,37]; similar mechanisms may also occur in MM *n*-GaInP DHs. RTA'd MM *n*-GaInP DHs attain a 4 × longer τ_{TRPL} compared to *p*-type, implying that MM *n*-GaInP is less affected by SRH and surface recombination. This observation aligns with a previous report highlighting the lifetime discrepancy between n- and *p*-GaAs for a given TDD (>1 × 10^5 cm^{-2}) due to differences in carrier mobilities [26]. The lower mobility of minority holes in MM n-GaInP compared to minority electrons in MM *p*-GaInP leads to reduced interaction with dislocations. Both RTA'd MM *p*- and *n*-GaInP reached ~2 × longer τ_{TRPL} compared to their annealed LM counterparts with the same doping concentrations [30], implying a relatively minor role for dislocation-related recombination. Earlier radiation studies showed that InP and InP-rich alloys such as $Ga_{1-x}In_xP$ and $Ga_{1-x}In_xAs_yP_{1-y}$ have superior radiation tolerance and lower damage constants for minority carrier diffusion length than GaAs-related materials due to lower migration energies of In- and P-vacancies compared to Ga- and As-vacancies [49]. This suggests that In-rich MM GaInP may exhibit better defect tolerance than LM GaInP. Moreover, activation energies for annealing of major defect centers decreased with an increasing composition of InP [49], which provides a possible explanation for the larger RTA improvement in MM GaInP compared to LM GaInP (Table I). The higher τ_{TRPL} and trend of increasing carrier mobility [50] with increasing indium composition make MM 1.7 eV GaInP promising for high-efficiency solar cells despite the elevated TDD.

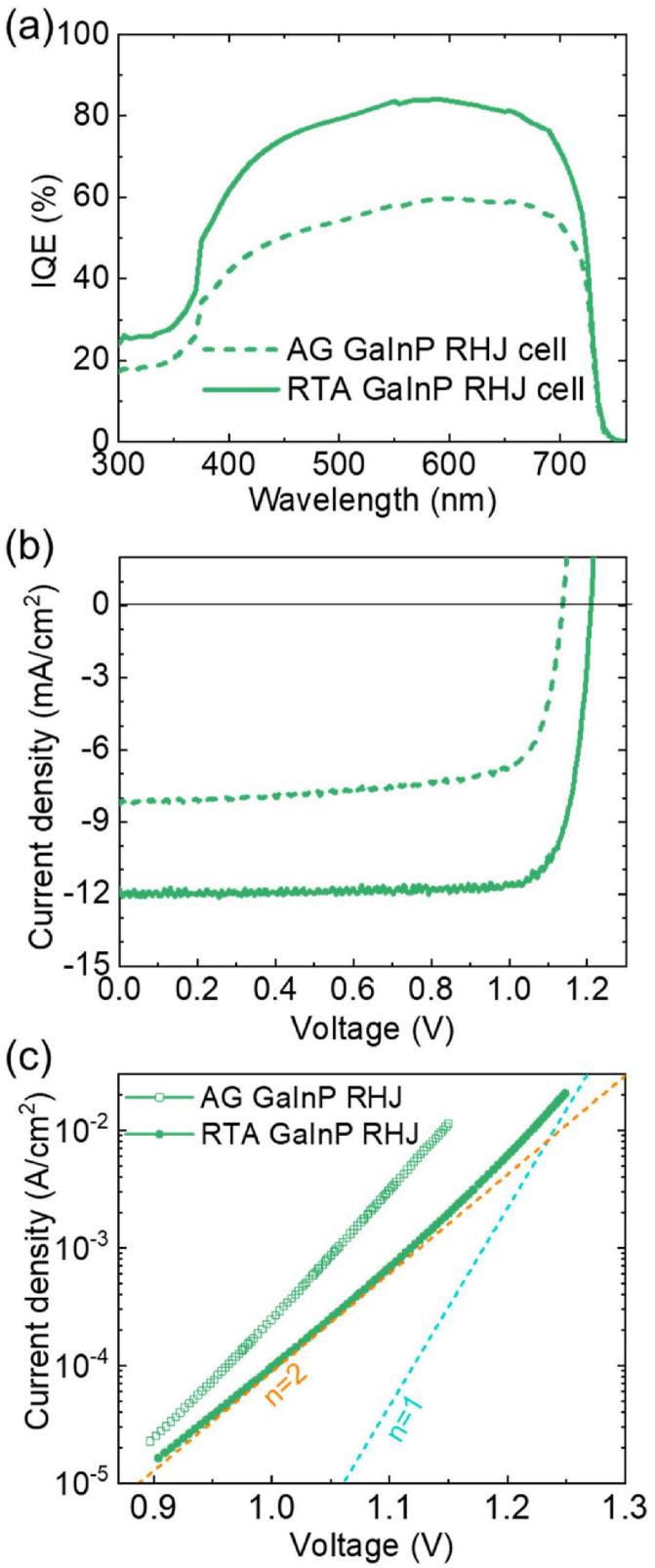

Fig. 5. (A) IQE, (b) LIV, and (c) Suns-V_{OC} curves of uncoated MM GaInP RHJ cells before and after RTA. RTA condition of all cells: 850 °C for 30s.

3.2. Eliminating majority hole blocking in RHJ cells

Fig. 4(a) and (b) show band diagrams and growth structures of our initial RHJ cells without the bridge layer (RHJ-1) and the redesigned

Table 3
Parameters of LM and MM GaInP FJ and RHJ cells.

Sample	RTA	J_{SC} (mA/cm^2)	V_{OC} (V)	W_{OC} (V)	pFF (%)	FF (%)	Efficiency (%)	J_{01} (A/cm^2)	J_{02} (A/cm^2)
MM GaInP RHJ cells	AG	8.25	1.137	0.545	85.0	72.5	6.80	3.05E-22	1.34E-12
	RTA	11.80	1.210	0.472	84.8	85.0	12.14	9.61E-24	4.22E-13
MM GaInP FJ cells	AG	12.17	1.119	0.558	86.0	81.8	11.23	1.17E-21	2.11E-12
	RTA	13.73	1.165	0.512	86.3	85.5	13.67	1.80E-22	5.15E-13
LM GaInP RHJ cells	AG	9.61	1.370	0.491	86.9	81.9	10.78	3.35E-26	1.59E-14
	RTA	10.17	1.420	0.442	85.8	84.7	12.23	3.88E-27	7.99E-15
LM GaInP FJ cells	AG	8.84	1.311	0.556	87.3	82.9	9.61	3.61E-25	4.52E-14
	RTA	10.36	1.401	0.493	87.6	86.3	12.52	1.39E-26	1.09E-14

RHJ cells with the bridge layer (RHJ-2), respectively. RHJ-1 suffers from a high R_s of 14.6 Ω-cm^2, resulting in a low FF of 68% despite a low W_{OC} (not shown); Suns-V_{OC} measurements gave a pseudo fill factor (pFF or FF without R_s) of 88%. TLM measurements of RHJ-1 gave reasonable R_{sheet} and $R_{contact}$ values of 832 Ω/sq and 0.0129 Ω-cm^2, leading us to hypothesize that majority hole blocking caused the high R_s and low FF. The 40 × difference in doping concentration and 1.1 eV change in E_g between MM AlGaInP BSF ($E_g = 2.3$ eV, $p_o = 1.0 \times 10^{17}$ cm^{-3}) and InGaAs spacer ($E_g = 1.2$ eV, $p_o = 4.0 \times 10^{18}$ cm^{-3}) lead to depletion at the heterointerface (Fig. 4 (a)) and hole blocking [51].

By introducing a heavily *p*-doped GaInP bridge layer and using an AlGaInP BSF with a lower E_g of 2.0 eV (Fig. 4(b)), the width of the majority hole-blocking barrier was reduced, resulting in a significant reduction in R_s from 14.6 to 1.1 Ω-cm^2 (Fig. 4(c) and Table II). Adding the bridge layer also reduced the difference between pFF and FF from 16.2 to 0.2%. FJ cells attained a low R_s of 0.46 Ω-cm^2 and a high FF of 85.5% without bridge layers due to a smaller difference in doping concentration between the buffer and BSF (Fig. 2(c)).

3.3. MM GaInP RHJ solar cells

Taking advantage of the long carrier lifetimes in lightly doped MM *n*-GaInP, we demonstrated the first MM 1.7 eV GaInP RHJ cells attaining low W_{OC} and high FF, which have the same design as RHJ-2 mentioned in section 3.2. After RTA at 850 °C for 30s, IQE increased across all wavelengths with a boost in peak IQE from 58% to 84.1% (Fig. 5(a)), indicating a significant enhancement in minority hole diffusion length. Despite the improvement, the annealed MM GaInP RHJ cells still have a lower IQE than our previously reported LM GaInP RHJ cells [30], which may originate from insufficient diffusion length and/or surface passivation.

The sloped LIV curve of unannealed RHJ cells near J_{SC} (Fig. 5(b)) shows that RHJ cells were significantly impacted by field-assisted carrier collection (FACC) [33] before RTA due to insufficient minority hole diffusion length; dark I–V curves were flat near the origin with high shunt resistance. RTA gave an absolute increase of 12.5% in FF and a rise in J_{MP}/J_{SC} from 0.84 to 0.96 by increasing minority hole diffusion length and eliminating FACC. The FF of the RTA'd RHJ cell reaches 85%, similar to previously reported 1.7 eV AlGaAs and GaInAsP cells [10,52,53]. Additionally, MM GaInP RHJ cells show an RTA enhancement in W_{OC} from 0.545 V to 0.472 V, comparable to the best MBE-grown LM GaInP RHJ cell (W_{OC} = 0.442 V) [30] though higher than the best MOCVD-grown 1.7 eV GaInAsP FJ cells ($W_{OC} = 0.390$ V) [1] due to the higher defect density in MBE-grown phosphides.

Suns-V_{OC} measurements revealed RTA decreased J_{01} and J_{02} in our RHJ cells by ~30 × and ~3 × , respectively (Fig. 5(c) and Table III), representing a more pronounced improvement in the quasi-neutral region than in the SCR. Although the low J_{01} value is desirable, the FF and V_{OC} of our MM GaInP RHJ cells remain limited by J_{02} due to the imbalanced RTA improvements between J_{01} and J_{02}. Further design optimization could boost cell performance by reducing recombination in the SCR and improving surface passivation.

3.4. MM GaInP FJ solar cells

RTA increased the IQE of MM GaInP FJ cells, particularly at wavelengths of 500–750 nm (Fig. 6(a)), due to a substantial improvement in minority electron diffusion length in the lightly doped *p*-type base. The peak IQE boosted from 85.4% to 94.3% after RTA, comparable to MOVPE-grown 1.7 eV GaInAsP cells [1] and MBE-grown LM GaInP FJ cells [30], despite dislocations. Based on the IQE, we estimate that the J_{SC} of our MM GaInP FJ cells could approach ~19 mA/cm^2 using an anti-reflection coating and low-shading grid design.

V_{OC} and FF of the MM GaInP FJ cells significantly increased after RTA (Fig. 6(b) and Table 3). RTA decreased the W_{OC} of MM GaInP FJ cells from 0.558 V to 0.512 V. In comparison, the LM cells in our previous work showed a larger RTA improvement in W_{OC} from 0.556 V to 0.493 V, potentially due to delta doping in the otherwise lightly doped emitter of the LM GaInP FJ cells; our previous work on LM GaInP FJ cells showed that a lightly doped emitter with delta spikes is preferable to a highly doped emitter with a uniform profile [30]. The FF of 85.5% in the annealed MM GaInP FJ cells is close to the pFF of 86.3% from suns-V_{OC}, indicating a low R_s. Unlike the RHJ cells, MM GaInP FJ cells exhibited no FACC and a high J_{MP}/J_{SC} of 0.93 before RTA due to the higher diffusivity of minority electrons in as-grown (AG) *p*-GaInP compared to minority holes in AG *n*-GaInP.

J_{01} and J_{02} values obtained from Suns-V_{OC} measurement decreased by ~7 × and ~4 × in FJ cells after RTA, indicating comparable improvements in both the quasi-neutral regions and SCR (Fig. 6(c) and Table III) [30]. Unlike the RHJ cells, MM FJ cells showed a transition from a J_{02}-dominated to a J_{01}-dominated regime near V_{MP} ~1.05 V, leading to slightly higher FF. Despite the non-negligible TDD, MM GaInP FJ cells showed comparable peak IQE, W_{OC}, and FF to LM GaInP FJ cells [30] due to longer lifetime and higher diffusivity in MM *p*-GaInP compared to the LM counterparts.

3.5. Comparison between MM RHJ and MM FJ GaInP solar cells

Even after RTA, MM GaInP RHJ cells exhibit lower IQE than FJ cells (Fig. 7(a)), likely due to low hole mobilities in *n*-GaInP [42,43] and insufficient minority hole lifetime. Although τ_{TRPL} in *n*-GaInP was 7 × longer than in *p*-GaInP, the ratio of electron to hole mobility is ~20–100, meaning that minority hole diffusion lengths in 1.7 eV *n*-GaInP may be significantly shorter than those in *p*-type material. While the absorber region of the FJ cell is significantly thicker than the RHJ cell, the primary benefit of the increased thickness (assuming adequate electron diffusion length) will only be seen at long wavelengths; in contrast, the IQE of the FJ cell exceeds that of the RHJ cell at all wavelengths. Our previous report showed that LM GaInP solar cells exhibit similar IQE for both FJ and RHJ designs [30], indicating that the MM GaInP RHJ cells in this work may have insufficient front-side surface passivation, causing lower peak IQE compared to MM GaInP FJ cells. We expect further optimization of the window layer doping profile could improve IQE in RHJ cells by suppressing surface recombination.

Unlike LM GaInP cells and 1.7 eV GaInAsP cells that use an indirect-gap, LM *n*-InAlP window [10,30], MM GaInP FJ and RHJ cells showed IQE losses at 450–550 nm (Fig. 7(a)) due to the use of a direct-gap, MM

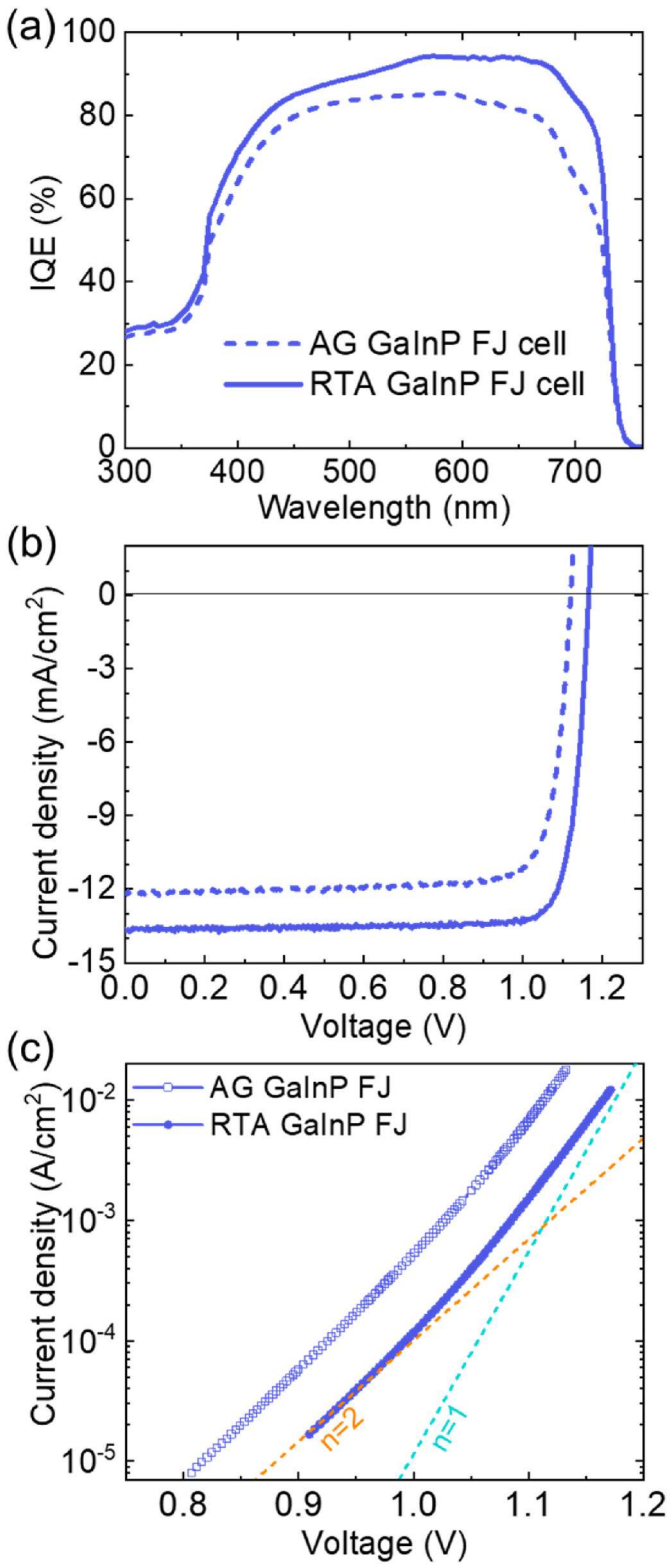

Fig. 6. (A) IQE, (b) LIV, and (c) Suns-V_{OC} curves of uncoated MM GaInP FJ cells before and after RTA. RTA condition of all cells: 850 °C for 30s.

n-InAlP window with E_g = 2.27 eV. A recent study reported that J_{SC} increased from 29.5 mA/cm^2 to 31.5 mA/cm^2 in GaAs cells using a tensile strained $In_{0.35}Al_{0.65}P$ window due to increased transparency [11]. We expect that using a tensile-strained, Al-rich $In_{0.48}Al_{0.52}P$ window layer [11,54] in our MM GaInP cells could reduce absorption from the window and improve J_{SC} by ~1 mA/cm^2.

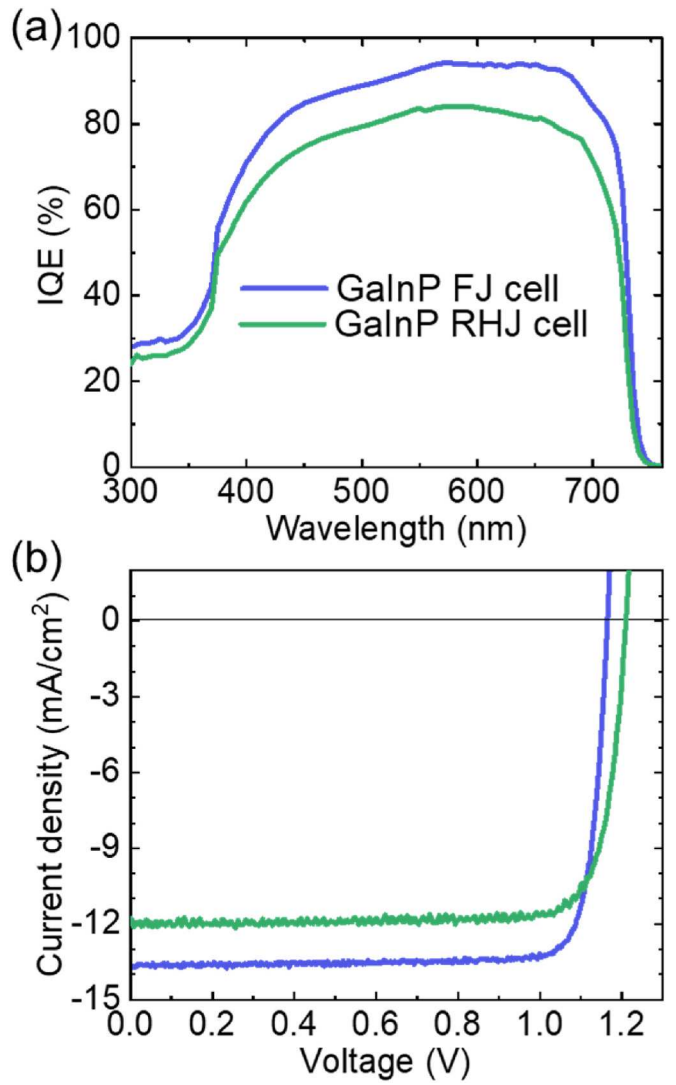

Fig. 7. (A) IQE and (c) LIV comparisons between MM GaInP RHJ and FJ cells after RTA.

Following the approach of Andre et al. [26], the expected V_{OC} values of MM GaInP FJ and RHJ cells for TDD of ~6 × 10^5 cm^{-2} may be estimated at 1.174 V and 1.251 V, respectively, in reasonable agreement with the measured values of 1.165 V and 1.210 V. MM GaInP RHJ cells show improved V_{OC} and lower $J_{01,02}$ values than MM GaInP FJ cells (Fig. 7(b) and Table III). The slight reduction in J_{02} of RHJ cells arises from the wider-E_g MM *p*-AlGaInP in the junction at the rear side of the device [31,40], which in turn reduces depletion region recombination. However, most of the W_{OC} benefit in the RHJ cells comes from the order of magnitude reduction in J_{01} in the RHJ cells compared to the FJ cells, which has also been observed in previous reports [30]. Despite the improved V_{OC}, the RHJ cell also suffers from a slightly reduced pFF due to its high ideality factor near V_{MP} arising from the ultra-low J_{01} value [33,55].

4. Conclusion

We presented the MBE growth and RTA effects of 1.7 eV MM GaInP cells with FJ and RHJ configurations. The τ_{TRPL} of 28 ns after RTA in 1.7 eV MM *n*-GaInP shows that long SRH lifetimes can be attained with a low TDD <1 × 10^6 cm^{-2}. Both 1.7 eV FJ and RHJ cells showed low W_{OC}, opening the possibility of achieving high efficiency, spectrally matched 1.7 eV (Al)GaInP/1.1 eV InGaAs tandem cells. We believe further

improvements in carrier collection in RHJ cells could be achieved by improving surface passivation and reducing parasitic optical loss in the direct-gap MM InAlP window. Despite the long lifetimes we observed in 1.7 eV *n*-GaInP, further improvements in hole diffusion length are still needed for RHJ cells to match the IQE of FJ cells in this absorber material.

CRediT authorship contribution statement

Mijung Kim: Writing – original draft, Methodology, Investigation, Conceptualization. **Yukun Sun:** Writing – review & editing, Investigation. **Ryan D. Hool:** Writing – review & editing, Investigation. **Minjoo Larry Lee:** Writing – review & editing, Project administration, Funding acquisition, Conceptualization.

Declaration of competing interest

The authors declare that they have no known competing financial interests or personal relationships that could have appeared to influence the work reported in this paper.

Data availability

Data will be made available on request.

Acknowledgments

M.K. was funded under NSF Grant No. 1810265. R.D.H. was supported by the NASA Space Technology Research Fellowship, Grants No. 80NSSC18K1174. Y.S. was funded under NSF Grants No. 1736181 and 1810265. This research was carried out in part in the Materials Research Laboratory Central Research Facilities, University of Illinois Urbana-Champaign.

References

[1] N. Jain, K.L. Schulte, J.F. Geisz, D.J. Friedman, R.M. France, E.E. Perl, A. G. Norman, H.L. Guthrey, M.A. Steiner, High-efficiency inverted metamorphic 1.7/1.1 eV GaInAsP/GaInAs dual-junction solar cells, Appl. Phys. Lett. 112 (2018), 053905.

[2] S. Fan, Z.J. Yu, R.D. Hool, P. Dhingra, W. Weigand, M. Kim, E.D. Ratta, B.D. Li, Y. Sun, Z.C. Holman, M.L. Lee, Current-matched III–V/Si epitaxial tandem solar cells with 25.0% efficiency, Cell Rep. Phys. Sci. 1 (2020), 100208.

[3] J.F. Geisz, J.M. Olson, D.J. Friedman, K.M. Jones, R.C. Reedy, M.J. Romero, Lattice-matched GaNPAs-on-silicon tandem solar cells, in: Conference Record of the Thirty-First IEEE Photovoltaic Specialists Conference, 2005, pp. 695–698.

[4] D.L. Lepkowski, T.J. Grassman, J.T. Boyer, D.J. Chmielewski, C. Yi, M.K. Juhl, A. H. Soeriyadi, N. Western, H. Mehrvarz, U. Römer, A. Ho-Baillie, C. Kerestes, D. Derkacs, S.G. Whipple, A.P. Stavrides, S.P. Bremner, S.A. Ringel, 23.4% monolithic epitaxial GaAsP/Si tandem solar cells and quantification of losses from threading dislocations, Sol. Energy Mater. Sol. Cell. 230 (2021), 111299.

[5] J.M. Olson, S.R. Kurtz, A.E. Kibbler, P. Faine, A 27.3% efficient $Ga_{0.5}In_{0.5}P$/GaAs tandem solar cell, Appl. Phys. Lett. 56 (1990) 623–625.

[6] T. Takamoto, E. Ikeda, H. Kurita, M. Ohmori, Over 30% efficient InGaP/GaAs tandem solar cells, Appl. Phys. Lett. 70 (1997) 381–383.

[7] J.F. Geisz, D.J. Friedman III, N V semiconductors for solar photovoltaic applications, Semicond. Sci. Technol. 17 (2002) 769–777.

[8] R.R. King, D.C. Law, K.M. Edmondson, C.M. Fetzer, G.S. Kinsey, H. Yoon, R. A. Sherif, N.H. Karam, 40% efficient metamorphic GaInP/GaInAs/Ge multijunction solar cells, Appl. Phys. Lett. 90 (2007), 183516.

[9] N.H. Karam, R.R. King, M. Haddad, J.H. Ermer, H. Yoon, H.L. Cotal, R. Sudharsanan, J.W. Eldredge, K. Edmondson, D.E. Joslin, D.D. Krut, M. Takahashi, W. Nishikawa, M. Gillanders, J. Granata, P. Hebert, B.T. Cavicchi, D. R. Lillington, Recent developments in high-efficiency $Ga_{0.5}In_{0.5}P$/GaAs/Ge dual- and triple-junction solar cells: steps to next-generation PV cells, Sol. Energy Mater. Sol. Cell. 66 (2001) 453–466.

[10] N. Jain, J.F. Geisz, R.M. France, A.G. Norman, M.A. Steiner, Enhanced current collection in 1.7 eV GaInAsP solar cells grown on GaAs by metalorganic vapor phase epitaxy, IEEE J. Photovoltaics 7 (2017) 927–933.

[11] M.A. Steiner, R.M. France, J. Buencuerpo, J.F. Geisz, M.P. Nielsen, A. Pusch, W. J. Olavarria, M. Young, N.J. Ekins-Daukes, High efficiency inverted GaAs and GaInP/GaAs solar cells with strain-balanced GaInAs/GaAsP quantum wells, Adv. Energy Mater. 11 (2021), 2002874.

[12] C.-W. Cheng, K.-T. Shiu, N. Li, S.-J. Han, L. Shi, D.K. Sadana, Epitaxial lift-off process for gallium arsenide substrate reuse and flexible electronics, Nat. Commun. 4 (2013) 1577.

[13] K. Lee, J.D. Zimmerman, X. Xiao, K. Sun, S.R. Forrest, Reuse of GaAs substrates for epitaxial lift-off by employing protection layers, J. Appl. Phys. 111 (2012), 033527.

[14] W. Guter, J. Schöne, S.P. Philipps, M. Steiner, G. Siefer, A. Wekkeli, E. Welser, E. Oliva, A.W. Bett, F. Dimroth, Current-matched triple-junction solar cell reaching 41.1% conversion efficiency under concentrated sunlight, Appl. Phys. Lett. 94 (2009), 223504.

[15] F. Dimroth, W. Guter, J. Schöne, E. Welser, M. Steiner, E. Oliva, A. Wekkeli, G. Siefer, S.P. Philipps, A.W. Bett, Metamorphic GaInP/GaInAs/Ge triple-junction solar cells with ≫ 41 % efficiency, in: 2009 34th IEEE Photovoltaic Specialists Conference, PVSC, 2009, 001038-001042.

[16] R.M. France, J.F. Geisz, M.A. Steiner, B. To, M.J. Romero, W.J. Olavarria, R. R. King, Reduction of crosshatch roughness and threading dislocation density in metamorphic GaInP buffers and GaInAs solar cells, J. Appl. Phys. 111 (2012), 103528.

[17] E.A. Fitzgerald, Y.H. Xie, D. Monroe, P.J. Silverman, J.M. Kuo, A.R. Kortan, F. A. Thiel, B.E. Weir, Relaxed Ge_xSi_{1-x} structures for III–V integration with Si and high mobility two-dimensional electron gases in Si, J. Vac. Sci. Technol., B: Microelectron. Process. Phenom. 10 (1992) 1807–1819.

[18] K.E. Lee, E.A. Fitzgerald, High-quality metamorphic compositionally graded InGaAs buffers, J. Cryst. Growth 312 (2010) 250–257.

[19] F. Romanato, E. Napolitani, A. Carnera, A.V. Drigo, L. Lazzarini, G. Salviati, C. Ferrari, A. Bosacchi, S. Franchi, Strain relaxation in graded composition $In_xGa_{1-x}As$/GaAs buffer layers, J. Appl. Phys. 86 (1999) 4748–4755.

[20] R. Kumar, A. Bag, P. Mukhopadhyay, S. Das, D. Biswas, Comparison of different grading schemes in InGaAs metamorphic buffers on GaAs substrate: tilt dependence on cross-hatch irregularities, Appl. Surf. Sci. 357 (2015) 922–930.

[21] K. Swaminathan, T.J. Grassman, L.-M. Yang, Q. Gu, M.J. Mills, S.A. Ringel, Optically-aligned visible/near-infrared dual-band photodetector materials and devices on GaAs using metamorphic epitaxy, J. Appl. Phys. 110 (2011), 063109.

[22] A. Bosacchi, A.C. De Riccardis, P. Frigeri, S. Franchi, C. Ferrari, S. Gennari, L. Lazzarini, L. Nasi, G. Salviati, A.V. Drigo, F. Romanato, Continuously graded buffers for InGaAsGaAs structures grown on GaAs, J. Cryst. Growth 175 (1997) 1009–1015.

[23] N.J. Quitoriano, E.A. Fitzgerald, Relaxed, high-quality InP on GaAs by using InGaAs and InGaP graded buffers to avoid phase separation, J. Appl. Phys. 102 (2007), 033511.

[24] M. Yamaguchi, C. Amano, Y. Itoh, Numerical analysis for high-efficiency GaAs solar cells fabricated on Si substrates, J. Appl. Phys. 66 (1989) 915–919.

[25] C. Donolato, Modeling the effect of dislocations on the minority carrier diffusion length of a semiconductor, J. Appl. Phys. 84 (1998) 2656–2664.

[26] C.L. Andre, D.M. Wilt, A.J. Pitera, M.L. Lee, E.A. Fitzgerald, S.A. Ringel, Impact of dislocation densities on n+/p and p+/n junction GaAs diodes and solar cells on SiGe virtual substrates, J. Appl. Phys. 98 (2005), 014502.

[27] S. Fan, Z.J. Yu, Y. Sun, W. Weigand, P. Dhingra, M. Kim, R.D. Hool, E.D. Ratta, Z. C. Holman, M.L. Lee, 20%-efficient epitaxial GaAsP/Si tandem solar cells, Sol. Energy Mater. Sol. Cell. 202 (2019), 110144.

[28] J.F. Geisz, R.M. France, K.L. Schulte, M.A. Steiner, A.G. Norman, H.L. Guthrey, M. R. Young, T. Song, T. Moriarty, Six-junction III–V solar cells with 47.1% conversion efficiency under 143 Suns concentration, Nat. Energy 5 (2020) 326–335.

[29] S. Lu, L. Ji, W. He, P. Dai, H. Yang, M. Arimochi, H. Yoshida, S. Uchida, M. Ikeda, High-efficiency GaAs and GaInP solar cells grown by all solid-state molecular-beam-epitaxy, Nanoscale Res. Lett. 6 (2011) 576.

[30] Y. Sun, B.D. Li, R.D. Hool, S. Fan, M. Kim, M.L. Lee, Improving the performance of GaInP solar cells through rapid thermal annealing and delta doping, Sol. Energy Mater. Sol. Cell. 241 (2022), 111725.

[31] M. Hinojosa, I. García, I. Rey-Stolle, C. Algora, Inverted rear-heterojunction GaInP solar cells using Te memory effect, Sol. Energy Mater. Sol. Cell. 205 (2020), 110235.

[32] T. Iwamoto, K. Mori, M. Mizuta, H. Kukimoto, Doped InGaP grown by MOVPE on GaAs, J. Cryst. Growth 68 (1984) 27–31.

[33] Y. Sun, S. Fan, J. Faucher, R.D. Hool, B.D. Li, P. Dhingra, M.L. Lee, 2.0–2.2 eV AlGaInP solar cells grown by molecular beam epitaxy, Sol. Energy Mater. Sol. Cell. 219 (2021), 110774.

[34] A. Tukiainen, J. Dekker, N. Xiang, M. Pessa, Effects of rapid thermal annealing on deep levels in n-GaInP, Phys. Scripta T114 (2004) 9.

[35] N. Xiang, A. Tukiainen, J. Dekker, J. Likonen, M. Pessa, Oxygen-related deep level defects in solid-source MBE grown GaInP, J. Cryst. Growth 227 (2001) 244–248.

[36] J. Dekker, A. Tukiainen, N. Xiang, S. Orsila, M. Saarinen, M. Toivonen, M. Pessa, N. Tkachenko, H. Lemmetyinen, Annealing of the deep recombination center in GaInP/AlGaInP quantum wells grown by solid-source molecular beam epitaxy, J. Appl. Phys. 86 (1999) 3709–3713.

[37] J.H. Kim, S.J. Jo, J.W. Kim, J.-I. Song, Characterization of deep levels in InGaP grown by compound-source molecular beam epitaxy, J. Appl. Phys. 89 (2001) 4407–4409.

[38] E.C. Paloura, A. Ginoudi, G. Kiriakidis, A. Christou, Effect of doping on electron traps in metalorganic molecular-beam epitaxial $Ga_xIn_{1-x}P$/GaAs heterostructures, Appl. Phys. Lett. 59 (1991) 3127–3129.

[39] A. Tukiainen, J. Dekker, T. Leinonen, M. Pessa, Characterization of deep levels in rapid-thermal-annealed AlGaInP, Mater. Sci. Eng., B 91 (2002) 389–392.

[40] J.F. Geisz, M.A. Steiner, I. García, S.R. Kurtz, D.J. Friedman, Enhanced external radiative efficiency for 20.8% efficient single-junction GaInP solar cells, Appl. Phys. Lett. 103 (2013), 041118.

[41] Y. Sun, A. Perna, P. Bermel, Comparing front- and rear-junction GaInP photovoltaic devices through detailed numerical and analytical modeling, IEEE J. Photovoltaics 9 (2019) 437–445.
[42] T. Shitara, K. Eberl, Electronic properties of InGaP grown by solid-source molecular-beam epitaxy with a GaP decomposition source, Appl. Phys. Lett. 65 (1994) 356–358.
[43] M. Ikeda, K. Kaneko, Selenium and zinc doping in $Ga_{0.5}In_{0.5}P$ and $(Al_{0.5}Ga_{0.5})_{0.5}In_{0.5}P$ grown by metalorganic chemical vapor deposition, J. Appl. Phys. 66 (1989) 5285–5289.
[44] D.L. Lepkowski, T. Kasher, J.T. Boyer, D.J. Chmielewski, T.J. Grassman, S. A. Ringel, The critical role of AlInP window design in III–V rear-emitter solar cells, IEEE J. Photovoltaics 10 (2020) 758–764.
[45] J. Faucher, Y. Sun, D. Jung, D. Martin, T. Masuda, M.L. Lee, High-efficiency AlGaInP solar cells grown by molecular beam epitaxy, Appl. Phys. Lett. 109 (2016), 172105.
[46] T. Masuda, S. Tomasulo, J.R. Lang, M.L. Lee, Comparison of single junction AlGaInP and GaInP solar cells grown by molecular beam epitaxy, J. Appl. Phys. 117 (2015), 094504.
[47] M. Wolf, H. Rauschenbach, Series resistance effects on solar cell measurements, Adv. Energy Convers. 3 (1963) 455–479.
[48] E.E. Perl, D. Kuciauskas, J. Simon, D.J. Friedman, M.A. Steiner, Identification of the limiting factors for high-temperature GaAs, GaInP, and AlGaInP solar cells from device and carrier lifetime analysis, J. Appl. Phys. 122 (2017), 233102.
[49] M. Yamaguchi, A. Khan, N. Dharmarasu, Analysis for superior radiation resistance of InP-based solar cells, Sol. Energy Mater. Sol. Cell. 75 (2003) 285–291.
[50] H.M. Macksey, N.H. Jr, R.D. Dupuis, J.C. Campbell, G.W. Zack, Crystal synthesis, electrical properties, and spontaneous and stimulated photoluminescence of $In_{1-x}Ga_xP$:N grown from solution, J. Appl. Phys. 44 (1973) 1333–1341.
[51] K. Itaya, M. Ishikawa, G.-i. Hatakoshi, Current-voltage characteristics of p-p isotype InGaAlP/GaAs heterojunction with a large valence-band discontinuity, Jpn. J. Appl. Phys. 32 (1993) 1919.
[52] S. Heckelmann, D. Lackner, C. Karcher, F. Dimroth, A.W. Bett, Investigations on $Al_xGa_{1-x}As$ solar cells grown by MOVPE, IEEE J. Photovoltaics 5 (2015) 446–453.
[53] A. Ben Slimane, A. Michaud, O. Mauguin, X. Lafosse, A. Bercegol, L. Lombez, J.-C. Harmand, S. Collin, 1.73 eV AlGaAs/InGaP heterojunction solar cell grown by MBE with 18.7% efficiency, Prog. Photovoltaics Res. Appl. 28 (2020) 393–402.
[54] R.K. Jain, G.A. Landis, D.M. Wilt, D.J. Flood, Strained $In_{0.40}Al_{0.60}As$ window layers for indium phosphide solar cells, Appl. Phys. Lett. 64 (1994) 1708–1710.
[55] M.A. Green, Solar cell fill factors: general graph and empirical expressions, Solid State Electron. 24 (1981) 788–789.